Proceedings of the ASME 2020
Internal Combustion Engine Division Fall Technical Conference
ICEF2020
November 1-4, 2019, Denver, CO, USA

ICEF2020-3010

RCCI WITH HIGH REACTIVITY S8-ULSD BLEND AND LOW REACTIVITY N-BUTANOL

Valentin Soloiu[1], Cesar E. Carapia[1], Richard Smith III[1], Amanda Weaver[1], Levi Mckinney[1], David Mothershed[1], Drake Grall[1], Marcel Ilie[1], Mosfequr Rahman[1]

[1]Georgia Southern University, Statesboro, GA

ABSTRACT

A fuel blend consisting of 10% S8 by mass (a Fischer-Tropsch synthetic kerosene), and 90% ULSD (Ultra Low Sulfur Diesel) was investigated for their combustion characteristics and impact on emissions during RCCI (Reactivity Controlled Compression Ignition) combustion in a single cylinder experimental engine utilizing a 65% by mass n-butanol port fuel injection (PFI). RCCI is a dual fuel combustion strategy achieved with the introduction of a PFI fuel of the low-reactive n-butanol, and a direct injection (DI) of a high-reactivity blend (FT-BLEND) into an experimental diesel engine. The combustion analysis and emissions testing were conducted at 1500 RPM at an engine load of 5 bar IMEP (Indicated Mean Effective Pressure), and CA50 of 9° ATDC (After Top Dead Center); CDC (Conventional Diesel Combustion) and RCCI with 65Bu-35ULSD were utilized as the baseline for AHRR (Apparent Heat Release Rate), ringing and emissions comparisons. It was found during a preliminary investigation with a Constant Volume Combustion Chamber (CVCC) that the introduction of 10% by mass S8 into a mixture with 90% ULSD by mass only increased Derived Cetane Number (DCN) by 0.8, yet it was found to have a significant effect on the combustion characteristics of the fuel blend.

This led to the change in injection timing necessary for maintaining 65Bu-35F-T BLEND RCCI at a CA50 of 5° ATDC (After Top Dead Center) to be shifted 3° closer to TDC, thus affecting the Ringing Intensity (RI), Pressure Rise Rate, and heat release of the blend all to decrease. CDC was conducted with a primary injection of 14° BTDC at a rail pressure of 800 bar, all RCCI testing was conducted with 65% PFI of n-butanol by mass and 35% DI, to prevent knock, with a rail pressure of 600 bar and a pilot injection of 60° BTDC for 0.35 ms. 65Bu-35ULSD RCCI was conducted with a primary injection at 6° BTDC with neat ULSD#2, the fuel 65Bu-35F-T BLEND in RCCI had a primary injection at 3° BTDC to maintain CA50 at 9° ATDC. 65Bu-35ULSD RCCI experienced a NO_X and soot emissions decrease of 40.8% and 91.44% respectively in comparison to CDC. The fuel 65Bu-35F-T BLEND in RCCI exhibited an additional decrease of NO_X and soot of 32.9 and 5.3%, in comparison to 65Bu-35ULSD RCCI for an overall decrease in emissions of 73.7% and 96.71% respectively. Ringing Intensity followed a similar trend with reductions in RI for 65Bu-35ULSD RCCI decreasing only by 6.2% whereas 65Bu-35F-T BLEND had a decrease in RI of 76.6%. Although emissions for both RCCI fuels experienced a decrease in NO_X and soot in comparison to CDC, UHC and CO did increase as a result of RCCI. CO emissions for 65Bu-35ULSD RCCI and 65Bu-35F-T BLEND where increased from CDC by a factor of 5 and 4 respectively with UHC emissions rising from CDC by a factor of 3.4. The fuel 65Bu-35F-T BLEND had a higher combustion efficiency than 65Bu-35ULSD in RCCI at 91.2% due to lower CO emissions of the blend.

Keywords: RCCI, n-butanol, Emissions, Mie Scattering, Constant Volume Combustion Chamber, Ringing Intensity.

NOMENCLATURE

AFR	Air Fuel Ratio
AHRR	Apparent Heat Release
ATDC	After Top Dead Center
BTDC	Before Top Dead Center
BMEP	Break Mean Effective Pressure
CAD	Crank Angle Degree
CA10	Crank Angle Degree @ 10% mass burned
CA50	Crank Angle Degree @ 50% mass burned
CA90	Crank Angle Degree @ 90% mass burned
CRDI	Common Rail Direct Injection
CD	Combustion Delay
CDC	Conventional Diesel Combustion
CI	Compression Ignition
CN	Cetane Number
CO	Carbon Monoxide
COV	Coefficient of Variation
CVCC	Constant Volume Combustion Chamber
D	Engine Bore

DI	Direct Injection
Dv10	Largest Droplet Size of 10% of Fuel Spray
Dv50	Largest Droplet Size of 50% of Fuel Spray
Dv90	Largest Droplet Size of 90% of Fuel Spray
ECU	Engine Control Unit
EGR	Exhaust Gas Recirculation
EPA	Environmental Protection Agency
FT	Fischer-Tropsch
FTIR	Fourier Transform Spectroscopy
HC	Hydrocarbons
HCCI	Homogeneous Charge Compression Ignition
HHV	Higher Heating Value
HTHR	High Temperature Heat Release
ID	Ignition Delay
IMEP	Indicated Mean Effective Pressure
LHV	Lower Heating Value
LTC	Low Temperature Combustion
LTHR	Low Temperature Heat Release
N	Engine Speed
NTC	Negative Temperature Coefficient Region
NOx	Nitrogen oxides
PCCI	Partially premixed charge compression-ignition
PFI	Port Fuel Injection
PPRR	Peak Pressure Rise Rate
Re	Reynolds Number
RCCI	Reactivity Controlled Compression Ignition
RPM	Revolutions Per Minute
RI	Ringing Intensity
S	Stroke
SI	Spark Ignition
SMD	Sauter Mean Diameter
TA10	Temperature @ 10% mass vaporized
TA50	Temperature @ 10% mass vaporized
TA90	Temperature @ 90% mass vaporized
TGA-DTA	Thermogravimetric Analysis – Differential Thermal Analysis
T_W	Wall Temperature
UHC	Unburnt Hydrocarbons
ULSD	Ultra-Low Sulfur Diesel
ρ_A	In-cylinder gas density
λ_A	Thermal Conductivity
μ_A	Viscosity In-cylinder Gases

INTRODUCTION

Industries rely on the use of compression ignition engines for the transportation of goods, construction, and power generation. Compression ignition engines expel harmful emissions during their normal operation. The use of these engines has made a significant environmental impact via their gaseous pollutant emissions. These gaseous emissions cause diesel engines to be one of the largest contributors to gaseous pollutants worldwide [1]. Combatting this, the Environmental Protection Agency (EPA) have placed stricter emissions regulations on compression ignition engines with which manufacturers must comply [2]. One of the most common technologies used to comply with the EPA's regulations are aftertreatment filter systems. Such filters collect pollutants after combustion has taken place. An alternative method to aftertreatment systems, advanced combustion techniques allow the reduction of in-cylinder emissions formation. These techniques have the potential to achieve low temperature combustion (LTC), and are utilized to reduce both nitrogen oxides (NOx) and soot emissions simultaneously without the use of any aftertreatment systems, ([3],[4],[5],[6],[7],[8],[9],[10]).

Approaches to achieve LTC stem from the need to regulate in cylinder temperature to limit formation of NOx. Lower temperature combustion is desired as higher temperatures are required for nitric oxide reactions to form. During low temperature combustion, the temperature threshold needed to produce NOx is not present, thus reducing the formation of NOx [11].The common approach to achieve this desired effect is utilizing the combustion strategies of Homogeneous Charge Compression Ignition (HCCI), Premixed Charge Compression Ignition (PCCI) and Reactivity Controlled Compression Ignition (RCCI). Both PCCI and HCCI are both limited on the range of load in which they can operate, requiring high amounts of EGR when at larger loads to keep in-cylinder temperature to a minimum. HCCI requires a high mixing rate at the beginning of the combustion cycle causing the ignition control to be non-existent. This, in turn, causes knock and a raised ceiling for Pressure Rise Rates. PCCI's operation calls for early injections to combat early ignition. Because of these early injections when operating at high loads with high EGR, ignition delay increases and decreases the combustion efficiency of the engine. The limitations of these two methods lead to the emergence of RCCI strategies. RCCI uses a dual fuel, duel injection method using multiple injection events to achieve LTC. The implementation of Port Fuel Injections (PFI) of a low reactivity fuel, with singular or multiple direct injections (DI) of a high reactivity fuel allows RCCI to have greater control than its predecessors. RCCI allows a large array of loads to be used while having a lesser dependence on EGR. This is because the low reactivity fuel's injections expel a cooling effect on the cylinder, allowing the engine to stay in LTC longer.

Effective RCCI strategies include the early injection of the PFI fuel and dual injections of the high reactivity fuel later in the cycle. These injection timing windows raise the reactivity of the fuel in the squish region, closest to the cylinder's walls, where the second injection closer to TDC increases the reactivity in the center of the cylinder. Injection timing, duration, and fuel consumption varies with engines and operation conditions [13]. Soloiu et. al utilized dual direct injections with RCCI to achieve LTC with GTL fuel blends direct injections and port fuel injections of n-butanol. A 60% mass fraction of n-butanol was port fuel injected with 3 different direct injected GTL fuels, at an engine speed of 1500 RPM and 4,5, and 6 bar IMEP. All RCCI injection patterns reduced both soot and NOx by 90%, compared to CDC. Mechanical efficiency also increased by 3-4% in RCCI mode compared to CDC modes. The combinations of fuels and RCCI

injection patterns achieved low temperature combustion while emitting desirable emissions patterns [3].

The majority of RCCI studies have used mainly ULSD or Biodiesels as the DI fuel and gasoline or and alcohol as the PFI fuel. This study is investigating the addition of a high reactivity Fischer-Tropsch fuel to ULSD to create a more reactive blend of fuel for the DI fuel and n-butanol as the PFI fuel. The addition of the Fischer-Tropsch fuel creates a novel blend for which RCCI is more effective to further reduce gaseous emissions. The production of n-butanol has a reduced carbon footprint compared to fuels that are formed through the production and refinement of non-renewable fossil fuels. Compared to methanol and ethanol, n-butanol's low water absorption, low-corrosivity in pipelines, high calorific value, and overall better miscibility with ULSD makes it a prime fuel for RCCI optimization [12].

Fischer-Tropsch is a process for which synthetic fuels are created using synthesis gases (CO and H_2); they use natural gas or coal. The production of these fuels creates less of a strain on the world's quickly depleting fossil fuel reserves. These synthetic fuels have shown significant reductions in engine emissions when used in a diesel engine. FT fuels exhibit emissions reductions such as CO, total hydrocarbons (THC), and soot emissions, with no loss of engine efficiency, during their combustion in CI engines, with respect to emissions obtained from CDC ([14],[15],[16],[17],[18]). S8 is characterized by its high cetane number, low viscosity, low density, higher heat value, and increased reactivity. This increase leads to much shorter ignition delays compared to neat ULSD and reduced fuel combustion during CI engine operation. [19]. Desantes et. al found that fuel properties such as kinematic viscosity as well as density could have the most impact on engine combustion and efficiencies [20][21].

FUEL ANALYSIS

Physical and Physiochemical properties of the selected fuels

The physical, thermal, and physiochemical properties of selected fuels were investigated in order to illustrate how the operations of these fuels within the test engine will influence the performance and emissions output. Fuel properties results were obtained experimentally by the authors, the selected fuels are summarized in Table 1.

Table 1: Properties of the Selected Fuels

	100 ULSD	100 S8	F-T BLEND	n-butanol
HHV (MJ/kg)	45.1	51.9	46.7	36.4
LHV (MJ/kg)	41.1	47.2	42.5	33.1
DCN*	47.4	60.4	48.2	16.4
Avg. Ignition Delay (ms)	4.0	2.8	3.4	40.16
Avg Combustion Delay (ms)	5.9	4.0	5.0	81.25
Viscosity @ 40 C (cP)	2.52	1.3	2.32	2.0
DV (10) (uV/mg)	12.5	10.0	11.8	10.2
DV (50) (uV/mg)	40.1	30.0	35.9	29.6
DV (90) (uV/mg)	131.1	108.9	111.7	94.2
TA (10) (°C)	110.0	78.0	107.0	54.3
TA (50) (°C)	180.0	126.0	173.0	80.8
TA (90) (°C)	240.0	162.0	228.0	95.4

* Derived Cetane Number (DCN) obtained in the lab, utilizing a PAC CID 510 governed by ASTM standard method D7668-14a.

** All properties in Table 1 obtained from in-house equipment.

The Parr 1341 constant volume calorimeter (error 0.3%) was used to determine the specific energy content of the selected fuels. Energy content is needed for comparison of the reactivity between selected fuels. Neat S8 had the highest reactivity and energy content of all the fuels at 51.9MJ/kg. Blending a 10% by mass amount of S8 accounts for a 3.6% increase of energy content compared to neat ULSD. This difference can effectively increase the mechanical efficiency of the engine by allowing the injection timing to be closer to TDC reducing mechanical work lost during RCCI operation. A Brookfield DV II Pro rotational viscometer set at a spindle speed of 200 RPM, with the temperature ranging from 28° C to 90° C was used to measure the dynamic viscosity of each fuel. Measurements of dynamic viscosity have a profound affect based on the operation of injection equipment, droplet speed, spray penetration, and atomization. The viscosity is especially important at low temperatures where higher viscosity may lead to inadequate fuel atomization and injector performance [22]. The neat synthetic kerosene, S8 shows the lowest viscosity as shown in figure 1.

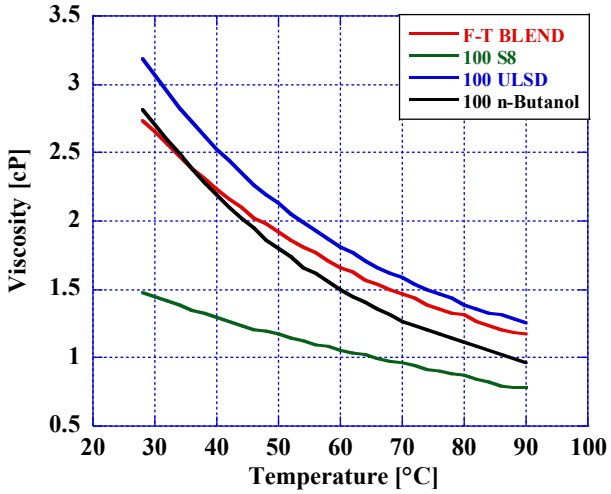

Figure 1: Viscosity of the Selected Fuels

The blend of S8 and ULSD displays a lower viscosity than neat ULSD, this lower viscosity is further enforced via the droplet distribution from the operation of a Malvern Mie scattering laser.

Low Temperature Oxidation analysis

A Differential Thermal Analysis (DTA) and a Thermogravimetric Analysis (TGA) measure respectively the energy release and vaporization rate of the selected fuels. The data collected was from a Shimadzu DTG-60 device (error of ±1.0%, accuracy ± 1.0 ˚C). The experimental combustion chamber was purged at a constant rate of 15 ml/min to simulate in-cylinder combustion conditions as well as temperatures required for homogeneous vaporization of fuel and local air. Temperature is controlled by incremental increase from 20˚C to 600˚C at a rate of 20˚C/min. The inert reference for each fuel is alumina, which loses little to no mass during testing. DTA is measured in the internal energy released and absorbed heat while TGA is the percent mass change of the fuels' vapor in reference to the baseline alumina during the test.

The TGA curve, analyzed in figure 2, illustrates the indicated vaporization rate of the fuel in a hot environment, such as during engine operation. The four selected fuels were analyzed by mass at 10%, 50%, and 90% vaporization. (TA10, TA50, TA90). Results are displayed in table 2, the TA 10, 50, and 90, of the S8 and ULSD fuel blend sample, vaporized at a lower temperature than neat ULSD. The S8 curve illustrates the reactivity the fuel sample. A 10% blend can increase reactivity of the directly injected high-reactivity charge utilized in this combustion study.

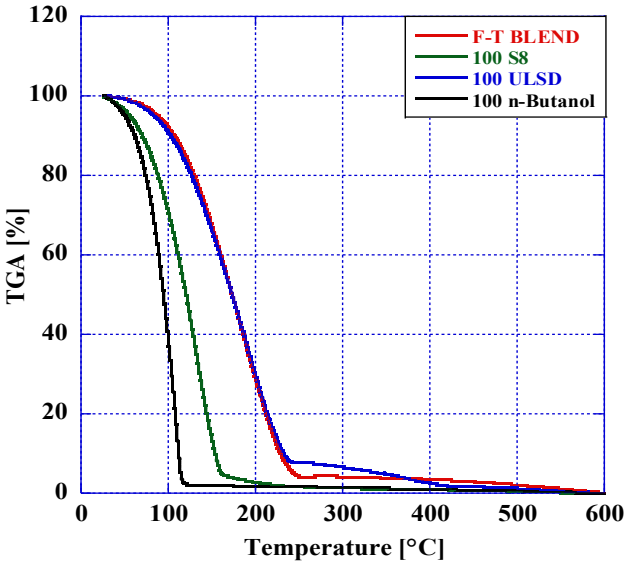

Figure 2: TGA Analysis of the Selected Fuels

Table 2: TA% Mass of Fuel Vaporized

TA%	100 ULSD	100 S8	F-T BLEND	n-butanol
TA (10)	110.0°C	78.0°C	107.0°C	54.3°C
TA (50)	180.0°C	126.0°C	173.0°C	80.8°C
TA (90)	240.0°C	162.0°C	228.0°C	95.4°C

Differential Thermal Analysis

The DTA is the analyzation of exothermic and endothermic reactions of the selected fuels within an environment of increasing temperature. Positive and negative slopes on the DTA curve in figure 3 indicate exothermic and endothermic reactions respectively. DTA measures reaction energy using change in voltage readings from thermocouples inside the test chamber. The curves in figure 3 are used to identify the Low Temperature Heat Release (LTHR). The maximum endothermic reaction for ULSD occurred at 180˚C, same with the blend. However, the blend releases all its energy more effectively than ULSD, hence the flatter curve after the initial reaction until the 600˚C mark. This is because neat S8 is very reactive and all its energy is expelled at 140˚C without more subsequent reactions.

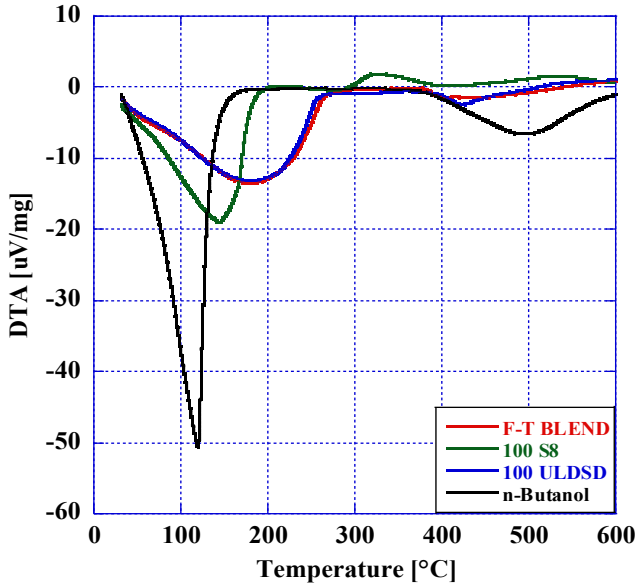

Figure 3: DTA Analysis of the Selected Fuels

Mie scattering HeNe laser analysis of spray development

Spray analysis was conducted using a Malvern Mie scattering 10mm beam diameter, Helium-Neon laser, utilizing Spraytech software. Spraytech Mie scattering software calculates Sauter Mean Diameter (SMD) and volume spray distribution by using Mie Scattering theory. The He-Ne laser projects a 632.8 nm wavelength laser beam through its control volume and optical system. The witness fuel injector, a single hole pintle type injector, is set 100mm away from the beam of the laser. The test injector injects an exact amount of fuel per each injection for each of the test fuels. Those fuel droplets in the spray scatter the light transmitted by the laser which is then observed by the detector array and processed with the Spraytech software. Collection of data begins at 1ms after the spray is detected by the laser, and the duration of the sampling is 5ms at a rate of 10 kHz. Each fuel spray is conducted at a fuel injector pressure of 180 bar, and enters the environment at ambient room temperature and atmospheric pressure[23]. Differences in spray pattern are due to the deviation in viscosity and vaporization for each fuel.

All three high reactivity fuels had a spray profile analysis conducted on them, the analysis included the volume frequency distribution and the Sauter Mean Diameter (SMD) over time for each fuel, as shown in figure 4 & 5. The peak in the spray volume distribution is the most frequent droplet size occurring each fuels spray distribution. Neat ULSD has the largest droplet sizes over S8 and the F-T BLEND, this can also be visualized by the viscosity of each fuels, ULSD is the most viscous at every temperature compared to the other two. These different viscosities and densities were found to correlate with the penetration the fuel spray has during operation of an experimental engine [21].

A spray pattern which has the lower sized droplet distribution at a higher concentration is desired, because it allows a higher surface area availability for more thorough combustion of the fuel. Figure 4 displays droplet size, in µm, Neat ULSD has the largest droplet diameter, and neat S8 has the smallest droplet diameter. These results are consistent with viscosity testing as the fuels with the highest viscosity have the largest SMD. The largest droplet size for each percent mass of fuel injected into the laser, denoted as DV10, 50, and 90, are displayed in table 3. Adding S8 to ULSD greatly reduces the droplet size percent by mass, at 10% the droplet size decreased by 5.6% compared to neat ULSD and by 90% mass the droplet size decreased by 14.7% more.

Table 3: Droplet Size Distribution % of Selected Fuels (µm)

Fuel	DV10	DV50	DV90
F-T BLEND	11.8	35.9	111.7
100 S8	10.0	30.0	108.9
100 ULSD	12.5	40.1	131.1

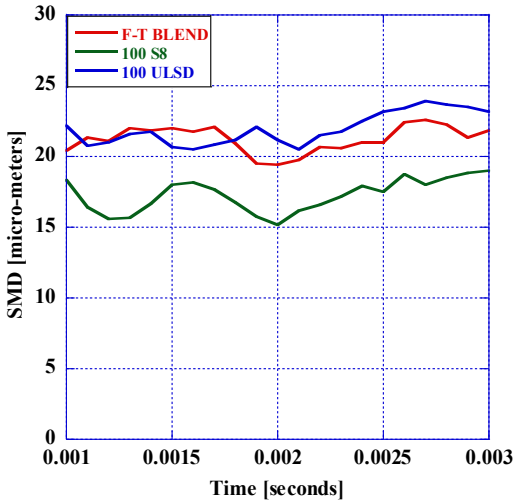

Figure 4: AVG SMD over Time

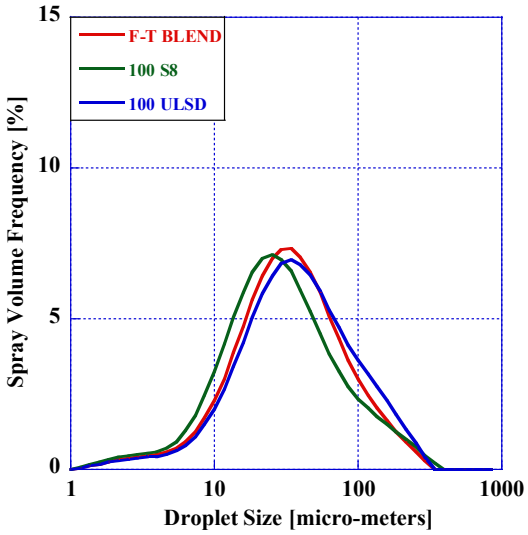

Figure 5: SMD Volume Distribution

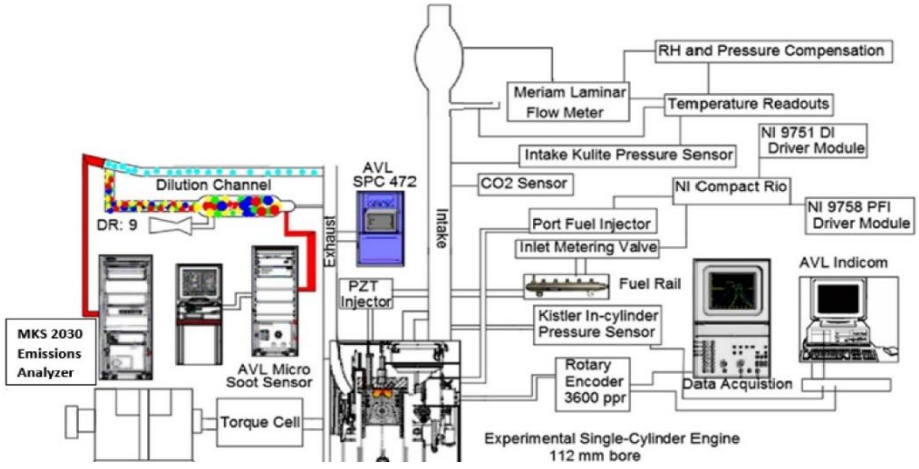

Figure 6: The Experimental Apparatus

EXPERIMENTAL APPARATUS

A single cylinder 1.1L experimental CI engine was utilized to perform a combustion/emissions study on a novel fuel mixture of 65Bu-35F-T BLEND in RCCI in comparison to both traditional RCCI and CDC. The specifications for the engine are listed in table 4 with the complete experimental apparatus shown in Figure 6. The engine utilized for this study has been outfitted with a Bosch CRDI system along with a custom injector nozzle tip to optimize the DI fuel spray with 7 orifices sized at 0.115 mm as seen in table 4.

TABLE 4: Engine Specifications

Peak Power	17kW @ 2200 RPM
Peak Torque	77.5 Nm @1400 RPM
Bore x Stroke	112 mm x 115 mm
Displacement	1.1L
Compression Ratio	16:1
Piston Geometry	Omega Bowl in piston
Piezo DI Injection Nozzle	7 orifices x 0.115mm
Cooling system	Water
Valves per cylinder	2
PFI pressure	2.8 bar
PFI Timing	20° CAD (340°BTDC in combustion)

In conjunction with the CRDI system, a PFI system was implemented as well for the injection of a secondary low reactive fuel, both system's fuel mass flow rates were measured utilizing a Maxx Machinery 213 piston flowmeter for the CRDI system and a P001 Model for the PFI system. The air intake was measured as well with a Meriam Z50MC-2 Laminar Flow meter, with corrections made to the measured value of air mass flow rate to consider the atmospheric pressure, humidity, and temperature.

In order to control several engine operating parameters a National Instruments Compact Rio 9076 Drivven ECU in conjunction with a NI 9751 module and a NI 9758 module controlled the DI system and PFI system respectively. The NI Drivven system in conjunction with an AVL INDICOM DAQ monitored combustion performance/phasing in real time (COV, PRR, IMEP, CA50), allowing for consistent engine operation. A hydraulic dynamometer applied a load on to the engine with an Omega TQ513 rotating torque load sensor attached in between to indicate the load applied. An Omron optical rotary encoder measured CAD with a resolution of 3600 pulses per rotation on the crankshaft and to synchronize the pressure data obtained from several pressure transducers. A Kistler 6053cc uncooled piezoelectric pressure transducer in series with a 5010B Dual-Mode Amplifier measured in-cylinder pressure. An Omega Px209 pressure transducer and Kulite ETL-175-190M pressure transducer measured exhaust and intake pressure respectively.

A Yokogawa DL850 high speed DAQ system with 125 cycles averaged per combustion test recorded both the pressure and CAD measurements for post processing. An NI 1.25 MS/s DAQ system recorded the air and fuel mass flow rates. This was done in concurrence with an MKS FTIR 20 gaseous species analyzer along with an AVL Model 483 Micro soot acoustic measurement device at a sampling rate of 1Hz over 2250 engine cycles.

EXPERIMENTAL METHODS

Both CDC and RCCI tests were conducted at an engine speed of 1500 RPM, with an engine load of 5 bar IMEP, and at a CA50 of 9° ATDC. The common rail pressure was maintained at 800 bar for CDC and 600 bar, with PFI at 65% fuel mass injected, for both RCCI tests. CDC utilized only one primary DI event, whereas RCCI tests conducted had two DI injection events, a pilot injection at 60° BTDC for a duration of 0.35 ms and the primary injection. Timing was changed per fuel to maintain CA50 at 9° ATDC with duration automatically changed by the ECU to maintain the set engine speed. The injection timing and duration are shown in Table 5.

TABLE 5: Injection Timing and Duration

	ULSD CDC	**65Bu-35ULSD RCCI**	**65Bu-35F-T BLEND**
SOI-1 timing	16° BTDC	60° BTDC	60° BTDC
SOI-1 duration	0.78 ms	0.35 ms	0.35 ms
SOI-2 timing	-	6° BTDC	3° BTDC
SOI-2 duration	-	0.32 ms	0.25 ms
PFI %	-	65%	65%
PFI Timing	-	20° CAD	20° CAD

The intake air was maintained at 32°C and COV was kept beneath 5% for all tests. This was done through both the manipulation of DI timing and maintaining PFI at 65% mass injected at an injection timing of 20° CAD to reduce exhaust scavenging (after exhaust valve closing). The global lambda for each combustion tests is shown in Table 6.

For RCCI combustion, two fuels were used in separate tests as the DI high-reactivity fuel, neat ULSD and F-T BLEND, with n-butanol chosen as the PFI low-reactivity fuel. The F-T BLEND fuel mixture consisted of 10% Fischer-Tropsch synthetic kerosene S8 and 90% ULSD by mass.

TABLE 6: Global Lambda at The Start of Combustion

Operation	**λ**
CDC	3.160
65Bu-35ULSD RCCI	3.214
65Bu-35F-T BLEND RCCI	3.155

COMBUSTION ANALYSIS

In Cylinder Combustion Pressure

The combustion pressure for all three combustion tests are shown in Figure 7, ULSD CDC in red, 65Bu-35ULSD RCCI in blue, and 65Bu-35F-T BLEND RCCI in green. A motoring curve (MC) was added with a black dotted line as a

reference for mechanical work. Both RCCI combustion studies utilized a 65% by mass n-butanol PFI and a 35% by mass DI of either neat ULSD or the F-T BLEND. For ULSD CDC, peak pressure was observed to be 72 bar @ 5° ATDC. ULSD RCCI achieved a peak pressure of 70 bar @ 8° ATDC resulting from the injection of the low reactivity fuel. Conversely, 65Bu-35F-T BLEND RCCI achieved a peak pressure of 72 bar @ 6° ATDC at a later injection timing that ULSD CDC. The significant change in the combustion characteristics of the 65Bu-35F-T BLEND RCCI can be attributed to the addition of the 10% S8 to the DI fuel as well as the homogeneous air/fuel charge. It was observed that although the DI fuel mixture for 65Bu-35F-T BLEND RCCI only consisted of 10% by mass S8, it had a profound effect on RCCI a obtaining a peak pressure of 72 bar @ 6° ATDC. 65Bu-35ULSD RCCI combustion only achieved a peak pressure of 70 bar @ 8° ATDC. ULSD CDC achieved the same peak pressure as 65Bu-35F-T BLEND RCCI of 72 bar @ 5° ATDC, as a result of both F-T BLEND's higher reactivity and the homogenous air/fuel charge. 65Bu-35F-T BLEND RCCI had a similar peak pressure timing to ULSD CDC despite the later injection timing of 65Bu-35F-T BLEND RCCI. 65Bu-35F-T BLEND RCCI had a smaller infliction occur for pressure rise rate than both ULSD CDC and 65Bu-35ULSD RCCI. However, 65Bu-35F-T BLEND RCCI had a more linear pressure rise rate as shown in the Pressure Rise Rate (PRR) section of this investigation. 65Bu-35ULSD RCCI had a greater delay than both ULSD CDC and 65Bu-35F-T BLEND RCCI with the initial rise in pressure occurring just after TDC in contrast to ULSD CDC and 65Bu-35F-T BLEND RCCI having pressure increase prior to TDC.

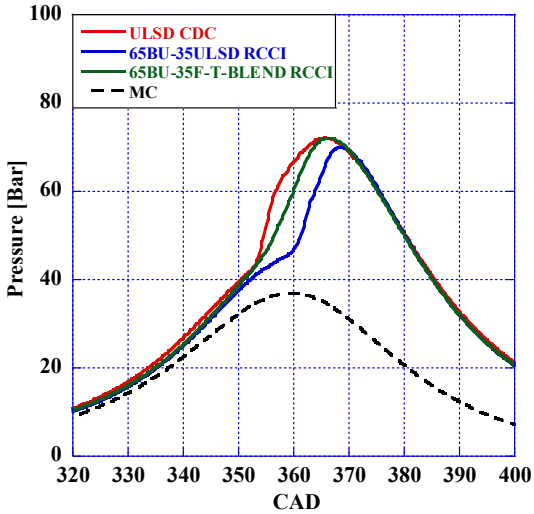

FIGURE 7: In-Cylinder Pressure

Figure 8 further confirms that both ULSD CDC and 65Bu-35F-T BLEND RCCI had their Peak Pressure Rise Rate (PPRR) occur prior to TDC with 65Bu-35ULSD RCCI occurring afterwards. ULSD CDC had a PPRR of 6.24 bar/CAD occurring at 4° BTDC whereas 65Bu-35ULSD RCCI had a similar PPRR at 6.04 bar/CAD occurring at 3° ATDC. While 65Bu-35ULSD RCCI had a similar PPRR to CDC, it had greater fluctuations past the peak value than CDC indicating regions of fuel combusting after the primary combustion event.

65Bu-35F-T BLEND RCCI had a 45% reduction in PPRR despite having a similar peak pressure as ULSD CDC. This show that despite the fuel mixture only containing 10% S8, the much higher reactivity of S8 (as observed in the CVCC) has beneficial combustion characteristics for RCCI with a potential for even greater emissions reduction.

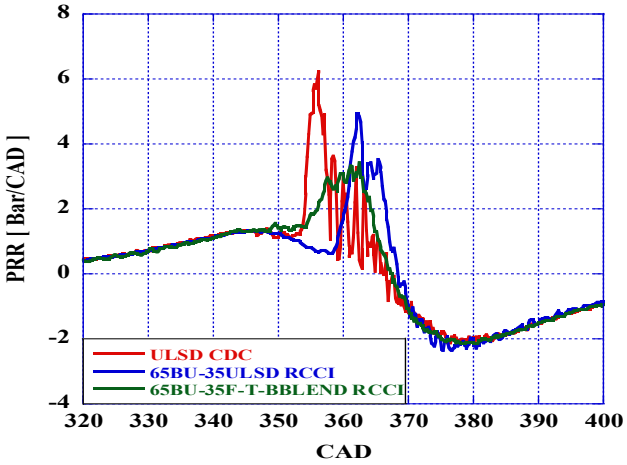

FIGURE 8: Pressure Rise Rate

Ringing Intensity

The RI for all three combustion tests is shown in Figure 9. In Eq.2, the constant β was set at 0.05 as obtained from literature review [25]. In figure 9 it is observed that 65Bu-35F-T BLEND RCCI had the greatest decrease in RI out of the three combustion tests. This is a direct result of the lower PPRR for 65Bu-35F-T BLEND RCCI , as it has the greatest influence on RI according to Eq.2.

$$RI = \frac{(\beta(\frac{dP}{dt})_{max})^2}{(2\gamma P_{max})}\sqrt{\gamma R T_{max}} \qquad (2)$$

As such, 65Bu-35F-T BLEND RCCI experienced a decrease in RI by 76.6% in comparison to ULSD CDC. 65Bu-35ULSD RCCI only had a reduction of RI of 5.7% signifying that 65Bu-35F-T BLEND RCCI had superior combustion stability over CDC and 65Bu-35ULSD RCCI.

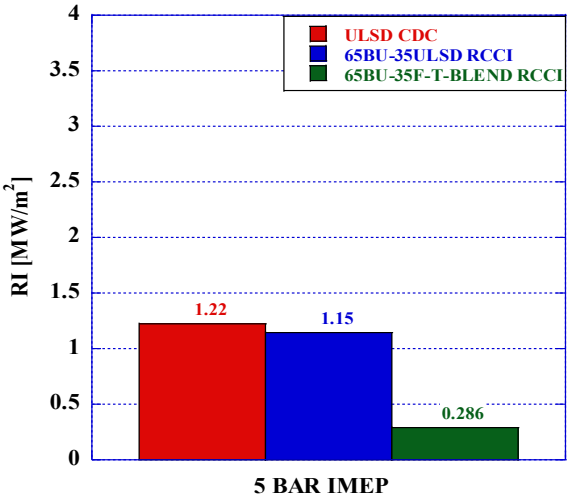

FIGURE 9: Ringing Intensity

Apparent Heat Release and MFB

The AHRR was obtained with the post-processing of the experimentally obtained pressure, temperature, and fuel data gathered by the various high speed DAQ systems mentioned previously. The first law of thermodynamics was applied to the data utilizing Eq.3 for the AHRR for each combustion test during the compression/power stroke of the engine. The air within the combustion chamber was treated as an ideal gas. Some corrections were made to the equation to consider the change in mass of the closed system due to DI. Blow-by was also taken into consideration and led to a loss of 2% mass in the combustion chamber as obtained from literature [3, 26].

$$\frac{dQ}{d\theta} = \frac{1}{[\gamma-1]} V \frac{dP}{d\theta} + \frac{\gamma}{[\gamma-1]} P \frac{dv}{d\theta} \quad (3)$$

Figure 10 contains the AHRR for each combustion test It was observed that 65Bu-35ULSD RCCI had the greatest peak AHRR in comparison to both CDC and 65Bu -5F-T BLEND RCCI at a value of 97 J/CAD. 65Bu-35ULSD RCCI exhibited a secondary peak in AHRR unlike the other 2 combustion tests, possibly attributed to a higher instability in combustion. This coupled with a similar RI to CDC could signify higher NVH characteristics than 65Bu-35F-T BLEND RCCI and should be investigated in a future study. Despite having a similar pressure trace, 65Bu 35F-T BLEND RCCI had a peak AHRR 27% lower than CDC at 64 J/CAD. This could be attributed to the extended combustion duration of 65Bu-35F-T BLEND RCCI in comparison to 65Bu-35ULSD RCCI that had a greater peak value but was done so for a shorter duration.

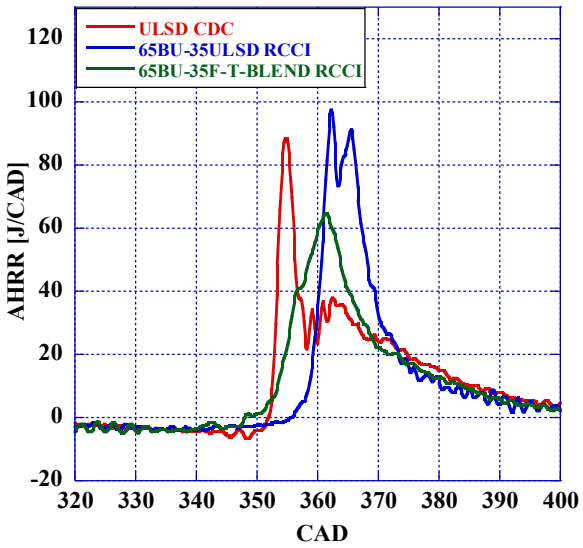

FIGURE 10: AHRR for CDC and RCCI

The results for MFB where compiled from the integration of AHRR and shown in Figure 11 with markers added for CA10, CA50, and CA90. Table 7 contains the location of CA10, CA50, and CA90 for all three tests as well. It was observed that RCCI tests decreased ID. The homogenous air/fuel mixture created by both PFI of n-butanol and priming of the combustion chamber with the pilot injection led to an initial rapid combustion in comparison to CDC. This was also observed in studies by Olmeda et. al [26]. 65Bu-35ULSD RCCI had a decrease in ID of 3° CAD in comparison to CDC. 65Bu-35F-T BLEND, however, had an apparent ID of 1° CAD. This is due to increased temperature/pressure causing combustion of the pilot injected fuel, resulting in pre-DI combustion.

The n-butanol, however, served as a regulator to this combustion and prevented dangerous knocking due to its low-reactivity. As a result, the primary injection event for 65Bu 35F-T BLEND RCCI was lower than 65Bu-35ULSD RCCI as less fuel was needed to maintain the engine speed at 1500 RPM with a load of 5 bar IMEP. Clearly, S8 has a great effect on 65Bu-35ULSD in RCCI combustion as the fuel mixture was only comprised of 10% S8 by mass, yet it greatly lowered ID and CD in comparison to 65Bu-35ULSD RCCI. 65Bu-35ULSD RCCI had a CD of 69° CAD with ULSD CDC only having a CD of 45° CAD, 65Bu-35F-T BLEND RCCI was able to decrease CD by 7° CAD. This decrease has the potential for increasing the combustion efficiency of the engine as less heat is lost to the engine block due to convection and radiation.

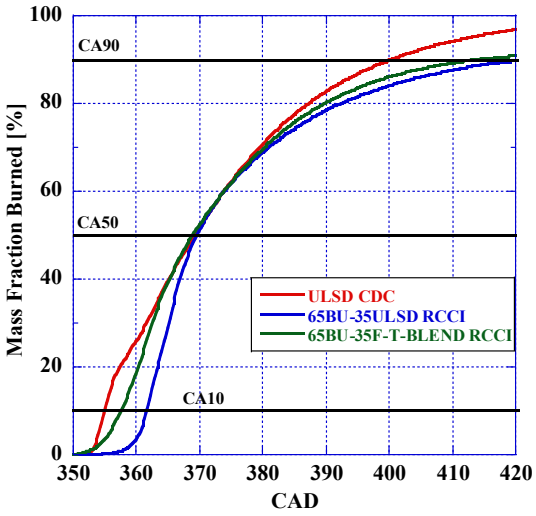

FIGURE 11: Mass Fraction Burned

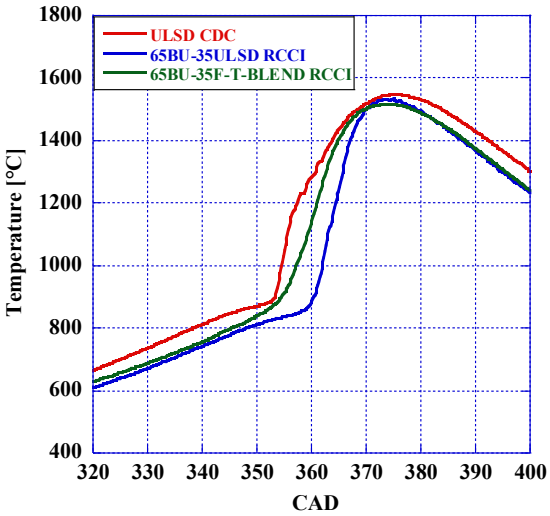

FIGURE 12: In-Cylinder Volume Averaged Combustion Temperature

Table 7: MFB, ID, and CD for 3 fuels

	ULSD CDC	65Bu 35ULSD RCCI	65Bu 35F-T BLEND RCCI
CA10	5° BTDC	1° ATDC	3° BTDC
CA50	9° ATDC	9° ATDC	8° ATDC
CA90	40° ATDC	70° ATDC	53° ATDC
ID	9 CAD	7 CAD	1 CAD
CD	45 CAD	69 CAD	56 CAD

Instantaneous Volume-Averaged Combustion Temperature

The pressure data was utilized for obtaining the combustion chamber's instantaneous average temperature and was sone so at each CAD increment, the results of which can be found in Figure 12. ULSD CDC had the highest temperature at 1547°C and was consistently higher than both RCCI tests. Both 65Bu-35ULSD RCCI and 65Bu-35F-T BLEND RCCI had a much lower initial in-cylinder temperature prior to combustion due to the cooling effect of n-butanol introduced in PFI. This led to a 50°C decrease to the air at the beginning of the compression stroke. As a result, 65Bu-35ULSD RCCI had a peak temperature of 1534°C, whereas 65Bu-35F-T BLEND RCCI was at 1517°C, the decrease in temperature for both RCCI tests could lead to promising NO_X reductions in comparison to CDC with the F-T BLEND having the greatest potential.

Emissions

An MKS FTIR 20 gaseous species analyzer along with an AVL Model 483 Micro soot acoustic measurement instrument recorded the exhaust emissions. Results for NO_X, soot, UHC, and CO can be found in Figures 13, 14, & 15, respectively. Soot emissions were lower for all RCCI tests with 65Bu-35F-T BLEND having the greatest decrease at 96.7% whereas 65Bu-35ULSD RCCI only had a 91.4% decrease. This demonstrates that S8 has a beneficial role in the reduction of soot emission in RCCI and the engine meets EPA tier 4 soot emissions.

NO_X emissions for 65Bu-35F-T BLEND RCCI also had a similar trend, as it had the greatest decrease in emissions resulting from its lower combustion temperatures. 65Bu-35F-T BLEND RCCI was able to decrease emissions by 73.7% in comparison to CDC, 65Bu-35ULSD RCCI on the other hand was only able to decrease it by 40%.

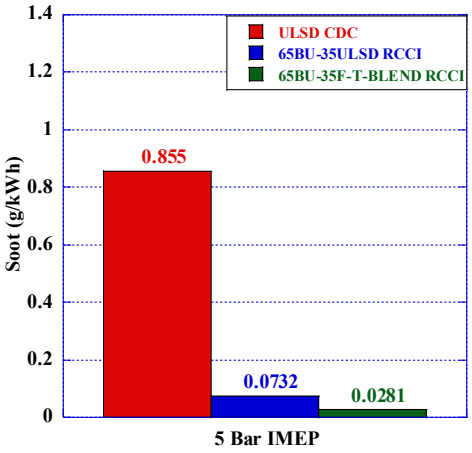

FIGURE 13: Soot Emissions

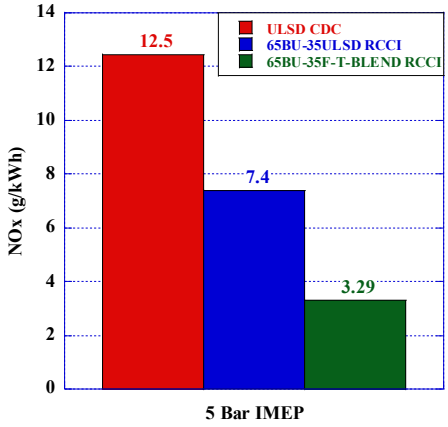

FIGURE 14: NO_X Emissions

However, both RCCI tests experienced a tradeoff for their reduction of NO_X and soot emissions with an increase in UHC emissions. Both RCCI methods experienced 3 times increase in UHC compared to CDC due to the n-butanol remaining unburnt near the crevices/walls of the combustion chamber. This, in turn, will lead to a decrease in combustion efficiency. Another indicator of combustion efficiency is the CO emissions emitted by a combustion process/fuel. As was observed in Figure 15, both RCCI combustion events had elevated CO emissions in comparison to CDC as a result of its dramatic reduction in both soot and NO_X emissions. 65Bu-35F-T BLEND RCCI had a smaller increase in CO emissions in comparison to 65Bu-35ULSD RCCI. 65Bu-35ULSD RCCI experienced an increase in CO emissions by a magnitude of 5.4, whereas 65Bu-35F-T BLEND RCCI only experienced a magnitude of 3.7. With all emissions in mind, S8 shows to be a promising additive to ULSD for RCCI combustion for the reduction of harmful NO_X and soot emissions whilst lowering CO emissions in comparison to traditional RCCI.

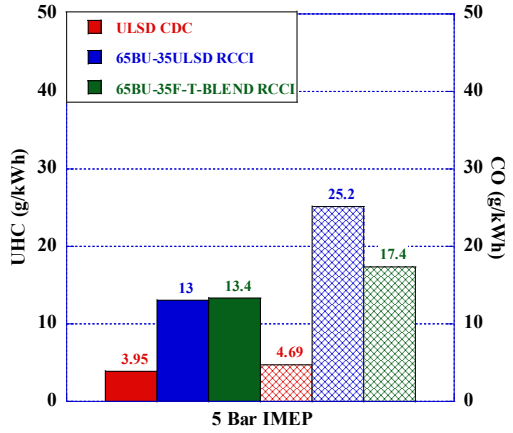

FIGURE 15: UHC Emissions

Combustion Efficiencies

Combustion efficiency was calculated utilizing the UHC, CO emissions, and LHV values of the fuels utilized as shown in Eq. 6. The results of which are shown in Figure 16, where it was shown that 65Bu-35ULSD RCCI had the lowest combustion efficiency. This was due to the increase in UHC and CO emissions in 65Bu-35ULSD RCCI due to fuel located in the crevices of the engine having incomplete combustion from PFI.

$$1 - \eta_c = \frac{\sum_i x_i Q_{Hv_t}}{\left[\dot{m}_f/(\dot{m}_a+\dot{m}_f)Q_{Hv_f}\right]} \quad (6)$$

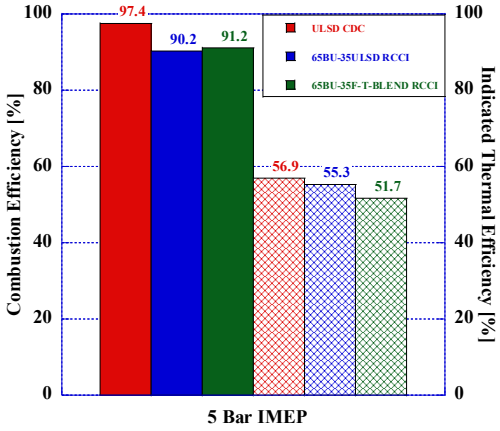

FIGURE 16: Combustion Efficiency

As a result, ULSD CDC had the highest combustion efficiency at 97.4%, however, 65Bu-35F-T BLEND RCCI had an increase in combustion efficiency of 1% over 65Bu-35ULSD RCCI from its reduction in CO emissions in comparison to 65Bu-35ULSD RCCI. This is due to S8's higher reactivity leading to the decrease in CD and therefore reduced the quantity of fuel unburnt from quenched combustion flames.

Indicated Thermal Efficiency

Indicated Thermal efficiency for all three combustion events are shown in Figure 16 where ULSD CDC had the highest efficiency at 56.9% in comparison to 65Bu-35ULSD RCCI at 55.3%. 65Bu-35F-T BLEND, despite having an increased combustion efficiency, experienced a decrease in thermal efficiency of 5.1%. This odd occurrence could be attributed to either the F-T BLEND having nearly the same UHC emissions as 65Bu-35ULSD RCCI despite it having injected less fuel than 65Bu-35ULSD RCCI. Having a higher LHV than neat diesel, or a greater combustion duration than 65Bu-35ULSD RCCI, leads to an increase in lost heat to the engine block also could have attributed to this occurrence. As a result, the fuel that was injected had a decreased thermal efficiency from the UHC not contributing to the work on the engine.

CONCLUSIONS

A fuel blend consisting of 10% S8 by mass (a Fischer-Tropsch synthetic kerosene), and 90% ULSD was investigated for its impact on emissions in RCCI combustion in a single cylinder experimental engine. The combustion analysis and emissions testing were conducted at 1500 RPM at an engine load of 5 bar IMEP, and CA50 of 9° ATDC; CDC and RCCI with ULSD #2 were utilized as the baseline for AHRR, ringing

and emissions comparisons. It was found in an investigation with a CVCC that the introduction of S8 into ULSD only increased DCN by 1.7%, yet it was found to have a significant effect on the combustion characteristics of the fuel blend.

This led to the change of injection timing necessary for maintaining 65Bu-35F-T BLEND RCCI at a CA50 of 9° ATDC to be shifted 3° closer to TDC, thus effecting the Ringing Intensity, Pressure Rise Rate, and heat release of the blend.

65Bu-35ULSD RCCI experienced a NO_X and soot emissions decrease of 40.8% and 91.44% respectively in comparison to CDC. The fuel F-T BLEND in RCCI exhibited an additional decrease of NO_X and soot of 32.9 and 5.3%, in comparison to 65Bu-35ULSD RCCI for an overall decrease in emissions of 73.7% and 96.71%, respectively. Ringing Intensity followed a similar trend with reductions in RI for 65Bu-35ULSD RCCI decreasing only by 6.2% whereas 65Bu-35F-T BLEND RCCI had a decrease in RI of 76.6%. Although emissions for both RCCI fuels experienced a decrease in NO_X and soot in comparison to CDC, UHC and CO did increase as a result of RCCI. CO emissions for 65Bu-35ULSD RCCI and 65Bu-35F-T BLEND were increased from CDC by a factor of 5.4 and 3.7 respectively with UHC emissions rising from CDC by a factor of 3.4. However, the fuel 65Bu-35F-T BLEND RCCI had a higher combustion efficiency than 65Bu-35ULSD in RCCI at 91.2% due to lower CO emissions of the blend. Thermal efficiency for 65Bu-35F-T BLEND RCCI experienced a decrease in comparison to 65Bu-35ULSD RCCI by 3.5% despite having less fuel consumption and CD than 65Bu-35ULSD RCCI. This decrease could be attributed to 65Bu-35F-T BLEND RCCI having similar UHC emissions to 65Bu-35ULSD RCCI. Thereby the fuel injected, despite having a higher LHV, produced the same UHC for the same quantity of work resulting in a decrease in thermal efficiency.

AKNOWLEDGMENTS

We would like to thank the College of Engineering Computing at Georgia Southern University for making this research possible through their funding of this project. The authors would like to acknowledge the support from Mike Smith of Exergy Engineering LLC, Janusz Waszkielewicz and Charles McGuffey from PAC, Daniel Stockton AVL, Mathew Viele of Vieletech, Joseph Wolfgang of Malvern, Richard Frazee from Singularity Scientific, Samuel Olesky from Kistler, Mastry Engine Center LLC, and Jon Palek from EMS. This paper was also jointly supported by the DoD and National Science Foundation under Grant no. 1950207.

Corresponding Author

*E-mail address: vsoloiu@georgiasouthern.edu

REFERENCES

[1] A. C. Lloyd and T. A. Cackette, "Diesel Engines: Environmental Impact and Control," *Journal of the Air & Waste Management Association*, vol. 51, no. 6, pp. 809–847, Dec. 2001.

[2] Environmental Protection Agency, 2005, "Control of Emissions of Air Pollution from New Motor Vehicles: In-Use Testing for Heavy-Duty Diesel Engines and Vehicles", OAR–2004–0072, Environmental Protection Agency.

[3] V. Soloiu, R. Gaubert, J. Moncada, J. Wiley, J. Williams, S. Harp, M. Ilie, G. Molina, and D. Mothershed, "Reactivity controlled compression ignition and low temperature combustion of Fischer-Tropsch Fuel Blended with n-butanol," *Renewable Energy*, vol. 134, pp. 1173–1189, Apr. 2019.

[4] V. Soloiu, J. D. Moncada, R. Gaubert, M. Muiños, S. Harp, M. Ilie, A. Zdanowicz, and G. Molina, "LTC (low-temperature combustion) analysis of PCCI (premixed charge compression ignition) with n-butanol and cotton seed biodiesel versus combustion and emissions characteristics of their binary mixtures," *Renewable Energy*, vol. 123, pp. 323–333, Aug. 2018.

[5] V. Soloiu, M. Duggan, S. Harp, B. Vlcek, and D. Williams, "PFI (port fuel injection) of n-butanol and direct injection of biodiesel to attain LTC (low-temperature combustion) for low-emissions idling in a compression engine," *Energy*, vol. 52, pp. 143–154, Apr. 2013.

[6] V. Chaudhari and D. Deshmukh, "Diesel and diesel-gasoline fuelled premixed low temperature combustion (LTC) engine mode for clean combustion," *Fuel*, vol. 266, p. 116982, Apr. 2020.

[7] H. Duan, M. Jia, Y. Chang, and H. Liu, "Experimental study on the influence of low-temperature combustion (LTC) mode and fuel properties on cyclic variations in a compression-ignition engine," *Fuel*, vol. 256, p. 115907, Nov. 2019.

[8] A. Jain, A. P. Singh, and A. K. Agarwal, "Effect of split fuel injection and EGR on NOx and PM emission reduction in a low temperature combustion (LTC) mode diesel engine," *Energy*, vol. 122, pp. 249–264, Mar. 2017.

[9] M. Krishnamoorthi, R. Malayalamurthi, Z. He, and S. Kandasamy, "A review on low temperature combustion engines: Performance, combustion and emission characteristics," *Renewable and Sustainable Energy Reviews*, vol. 116, p. 109404, Dec. 2019.

[10] R. Michikawauchi, S. Tanno, Y. Ito, and M. Kanda, "Combustion Improvement of Diesel Engine by Alcohol Addition - Investigation of Port Injection Method and Blended Fuel Method," *SAE International Journal of Fuels and Lubricants*, vol. 4, no. 1, pp. 48–57, Apr. 2011.

[11] L. Shi, W. Xiao, M. Li, L. Lou, and K.-Y. Deng, "Research on the effects of injection strategy on LTC combustion based

on two-stage fuel injection," *Energy*, vol. 121, pp. 21–31, Feb. 2017.

[12] K. Wadumesthrige, K. Y. S. Ng, and S. O. Salley, "Properties of Butanol-Biodiesel-ULSD Ternary Mixtures," *SAE International Journal of Fuels and Lubricants*, vol. 3, no. 2, pp. 660–670, Oct. 2010.

[13] R. D. Reitz and G. Duraisamy, "Review of high efficiency and clean reactivity controlled compression ignition (RCCI) combustion in internal combustion engines," *Progress in Energy and Combustion Science*, vol. 46, pp. 12–71, 2015.

[14] P. W. Schaberg, I. S. Myburgh, J. J. Botha, and I. A. Khalek, "Comparative Emissions Performance of Sasol Fischer-Tropsch Diesel Fuel in Current and Older Technology Heavy-Duty Engines," *SAE Technical Paper Series*, 2000.

[15] J. Czerwinski, Y. Zimmerli, T. Neubert, A. Heitzer, and M. Kasper, "Injection, Combustion and (Nano) Particle Emissions of a Modern HD-Diesel Engine With GTL, RME & amp; ROR," *SAE Technical Paper Series*, Jul. 2007.

[16] F. Payri, J. Arrègle, C. Fenollosa, G. Belot, A. Delage, P. Schaberg, I. Myburgh, and J. Botha, "Characterisation of the Injection-Combustion Process in a Common Rail D.I. Diesel Engine Running with Sasol Fischer-Tropsch Fuel," *SAE Technical Paper Series*, Jun. 2000.

[17] P. Schaberg, J. Botha, M. Schnell, H.-O. Hermann, N. Pelz, and R. Maly, "Emissions Performance of GTL Diesel Fuel and Blends with Optimized Engine Calibrations," *SAE Technical Paper Series*, May 2005.

[18] J. Krahl, G. Knothe, A. Munack, Y. Ruschel, O. Schröder, E. Hallier, G. Westphal, and J. Bünger, "Comparison of exhaust emissions and their mutagenicity from the combustion of biodiesel, vegetable oil, gas-to-liquid and petrodiesel fuels," *Fuel*, vol. 88, no. 6, pp. 1064–1069, Jun. 2009.

[19] A. Torregrosa, A. Broatch, B. Plá, and L. Mónico, "Impact of Fischer–Tropsch and biodiesel fuels on trade-offs between pollutant emissions and combustion noise in diesel engines," *Biomass and Bioenergy*, vol. 52, pp. 22–33, May 2013.

[20] Desantes José M., Payri Raúl, García Antonio, and J. Manin, "Experimental Study of Biodiesel Blends' Effects on Diesel Injection Processes," *Energy & Fuels*, vol. 23, no. 6, pp. 3227–3235, May 2009.

[21] D. Kim, J. Martz, and A. Violi, "Effects of fuel physical properties on direct injection spray and ignition behavior," *Fuel*, vol. 180, pp. 481–496, Sep. 2016.

[22] F. K. Tsuji and L. D. Neto, "Influence of Vegetable Oil in the Viscosity of Biodiesel – A Review," *SAE Technical Paper Series*, 2008. doi:10.4271/2008-36-0170

[23] V. Soloiu, J. T. Wiley, R. Gaubert, D. Mothershed, C. Carapia, R. C. Smith, J. Williams, M. Ilie, and M. Rahman, "Fischer-Tropsch coal-to-liquid fuel negative temperature coefficient region (NTC) and low-temperature heat release (LTHR) in a constant volume combustion chamber (CVCC)," *Energy*, vol. 198, p. 117288, May 2020.

[24] Soloiu, V., Moncada, J.D., Gaubert, R., Knowles, A., Molina, G., Ilie, M., Harp, S., Wiley, J.T., 2018. Reactivity Controlled Compression Ignition combustion and emissions using n-butanol and methyl oleate. Energy 165, 911–924. doi:10.1016/j.energy.2018.09.181

[25] Eng, J.A., 2002. Characterization of Pressure Waves in HCCI Combustion. SAE Technical Paper Series. doi:10.4271/2002-01-2859

[26] P. Olmeda, A. García, J. Monsalve-Serrano, and R. L. Sari, "Experimental investigation on RCCI heat transfer in a light-duty diesel engine with different fuels: Comparison versus conventional diesel combustion," Applied Thermal Engineering, vol. 144, pp. 424–436, 2018.